# Elastic properties and electronic structures of lanthanide hexaborides

Duan Jie(段 婕)[a], Zhou Tong (周 彤)[a], Zhang Li(张 莉)[a]†,
Du Ji-Guang(杜际广)[b], Jiang Gang(蒋 刚)[a], and Wang Hong-Bin(王宏斌)[a]

[a] *Institute of Atomic and Molecular Physics, Sichuan University, Chengdu* 610065, *China*
[b] *College of Physical Science and Technology, Sichuan University, Chengdu* 610065, *China*

(Received 22 January 2015; revised manuscript received 24 April 2015; published online 20 July 2015)

The structural, elastic, and electronic properties of a series of lanthanide hexaborides ($Ln$B$_6$) have been investigated by performing *ab initio* calculations based on the density functional theory using the Vienna *ab initio* simulation package. The calculated lattice and elastic constants of $Ln$B$_6$ are in good agreement with the available experimental data and other theoretical results. The polycrystalline Young's modulus, shear modulus, the ratio of bulk to shear modulus $B/G$, Poisson's ratios, Zener anisotropy factors, as well as the Debye temperature are calculated, and all of the properties display some regularity with increasing atomic number of lanthanide atoms, whereas anomalies are observed for EuB$_6$ and YbB$_6$. In addition, detailed electronic structure calculations are carried out to shed light on the peculiar elastic properties of $Ln$B$_6$. The total density of states demonstrates the existence of a pseudogap and indicates lower structure stability of EuB$_6$ and YbB$_6$ compared with others.

**Keywords:** elastic properties, electronic structure, *ab initio* calculations, thermodynamic properties

**PACS:** 62.20.D–, 71.15.–m, 31.15.A–, 05.70.–a **DOI:** 10.1088/1674-1056/24/9/096201

## 1. Introduction

Lanthanide hexaborides ($Ln$B$_6$: $Ln$ = La, Ce, Pr, Nd, Pm, Sm, Eu, Gd, Tb, Dy, Ho, Er, Tm, Yb, Lu) have attracted extensive experimental and theoretical interest due to their intriguing physical properties. For example, LaB$_6$ is a typical metal and becomes superconducting at $T_C = 0.45$ K,[1,2] CeB$_6$ is a dense Kondo material and shows heavy fermion behavior.[3] SmB$_6$, a typical mixed valence compound, has been theoretically proven to be a topological Kondo insulator, which is supported by recent photo emission and transport experiments.[4,5] YbB$_6$ is found to be a moderately correlated $Z_2$ topological insulator, similar to SmB$_6$ but having a much larger bulk band gap.[6] Furthermore, the lanthanide hexaborides are also considered as hard and refractory materials because of their special cage structure.[7] Bulk lanthanide hexaborides have low work functions ranging from 2.1 eV to 3.8 eV, which make them excellent candidate materials for electron emitter devices.[8] Moreover, they have been applied as scratch-resistant surface decorative coatings due to their tunable attractive colors. For instance, the stoichiometric LaB$_6$ is usually purple, while its color turns to deep blue when it is lanthanum deficient. Consequently, the investigation of the basis physical properties of a series of lanthanide hexaborides such as structural, elastic, and electronic properties is necessary and offers credible references for their various applications.

In general, the elastic properties of a solid are important because some physical properties, such as the bulk modulus, shear modulus, Young's modulus, and Poisson's ratio can be derived from the elastic constants.[9] Up to now, most studies have focused on the magnetic and thermodynamic properties of $Ln$B$_6$.[10] The structural and elastic properties of some $Ln$B$_6$ have also been investigated experimentally by several groups but their results are relatively contradictory or insufficient. Some significantly different values have been reported for the measured elastic constants of CeB$_6$, especially $C_{12}$; Takegahara *et al.*[11] gave $C_{12} = -93$ GPa while Nakamura *et al.*[12] reported a value of 53 GPa for the same constant. The bulk moduli also show small differences among the various experimental reports.[13] On the other hand, single crystal elastic constants for the $Ln$B$_6$ compounds are scarce due to the difficulties of the experiments. The elastic properties of a solid are also closely associated with various fundamental solid-state properties, such as phonon spectra, specific heat, Debye temperature, etc. In view of this, it is necessary and essential to obtain their elastic constants by the first-principles calculations.

As we all know, in the lanthanide series both Eu and Yb are divalent in the solid state while all of the others are in the trivalent state. There is a substantial energy penalty for Eu and Yb to be in the trivalent state. Consequently, systematics are observed for the trivalent *Ln* and their compounds in terms of crystal structures and physical properties, whereas anomalies are observed for Eu and Yb.[14] The abnormalities relating to Eu and Yb are probably due to their special electronic configurations. Eu has a half-filled 4f orbital and Yb has a completely

†Corresponding author. E-mail: lizhang@scu.edu.cn

filled 4f orbital; therefore, they have stable configurations of low energy. But their compounds disturb the stable electronic configurations through charge transfer or chemical bonding. The deviations will be seen repeatedly throughout this work.

The main objective of this paper is to study the regularity of elastic properties and electronic structure of the $Ln$B$_6$ compounds. This paper is organized as follows. The computational methodologies employed in the current study are given in Section 2. We present and discuss the results obtained and compare them with the available experimental and theoretical data in Section 3. Finally, the results are summarized in Section 4.

## 2. Theoretical and computational methods

Our first-principles electronic structure calculations are based on the density functional theory (DFT) in conjunction with projector augmented wave potentials (PAW)[15,16] within the generalized gradient approximations (GGA) of Perdew–Burke–Ernzerhof (PBE) as implemented in the Vienna *ab initio* simulation package (VASP).[17–20] Generally, the PAW potentials are more reliable than the ultra-soft pseudopotentials because of the smaller cut off radius and the more accurate valence electron wave functions in the nuclear area. The validity for the $Ln$B$_6$ binary compounds has been widely verified.[12] Two choices of potentials are available for each *Ln* element: a standard version in which the entire set of f levels are treated within the valence band and a divalent or trivalent version (e.g., $Yb^{2+}$ for Yb and $Pm^{3+}$ for Pm) in which some f electrons are kept frozen in the core. There are several exceptions: (i) there is only a standard potential available for La because it has no occupied f levels in its elemental state, and (ii) there is only a trivalent version of potential available for Tb, Dy, Ho, and Er with VASP. Furthermore, the previous studies of the ground state structures, formation energies, and elastic constants of the *Ln* elements and compounds[21] indicate that the *f* core approach is the correct method to treat the *Ln* elements when thermodynamic and elastic properties are of interest. In this work, pseudopotentials with the f electrons frozen in the core were used throughout. A plane-wave energy cutoff of 550 eV was taken for all $Ln$B$_6$. The $13\times13\times13$ *k*-points for $Ln$B$_6$ unit cell with the Monkhorst–Pack scheme were adopted for the Brillouin zone sampling. In all cases, the total energy of self-consistent convergence was $10^{-5}$ eV/cell and the process was terminated when the atomic force was less than $10^{-3}$ eV/Å. Spin polarization with ferromagnetic ordering was used in all calculations and we found that all the $Ln$B$_6$ considered here are not magnetic. To produce more accurate densities of states, a dense *k*-point mesh of $19\times19\times19$ was used, and the total DOS was computed by the Gaussian smearing method.[17–20] The chosen plane-wave cut off and numbers of *k* points have been tested carefully to ensure good converged results for all of the computations. The elastic constants were calculated through the energy strain method. The analysis of the density of states indicated the existence of a pseudogap.

## 3. Results and discussion

### 3.1. Structural stability and ground state properties

As illustrated in Fig. 1, the lanthanide hexaborides crystallize in cubic CsCl-type structure which belongs to the space group $O_h^1\left(Pm\bar{3}m\right)$.[13] The lanthanide atom is located at the 1*a* (0, 0, 0) Wyckoff position while the octahedral boron molecule B$_6$ is placed in the 6*f* Wyckoff position with relative coordinate (1/2, 1/2, *x*), where *x* is the positional parameter. The primitive unit cell contains seven atoms. The equilibrium lattice parameter $a_0$ has been computed by minimizing the crystal total energy by means of Murnaghan's equation of state (EOS).[22] Our calculated lattice parameter $a_0$ and internal position *x* along with related experimental and theoretical values are listed in Table 1. In our GGA calculations, the predicted lattice constant of LaB$_6$ is 4.1558 Å, which is in good agreement with the experimental data 4.1565 Å[10] and other theoretical results 4.1300 Å,[10] 4.1277 Å,[10] 4.1560 Å.[23] For CeB$_6$, the present optimized lattice parameter $a_0$ is 4.1585 Å in accordance with the experimental data 4.1410 Å.[23] For other $Ln$B$_6$, the results obtained are also comparable to their

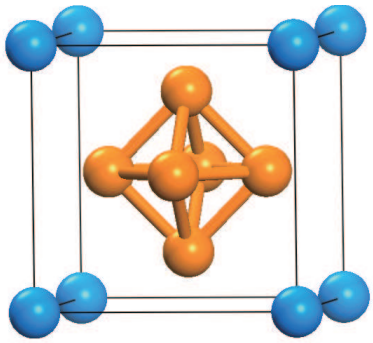

**Fig. 1.** (color online) Unit cell of lanthanide hexaboride ($Ln$B$_6$).

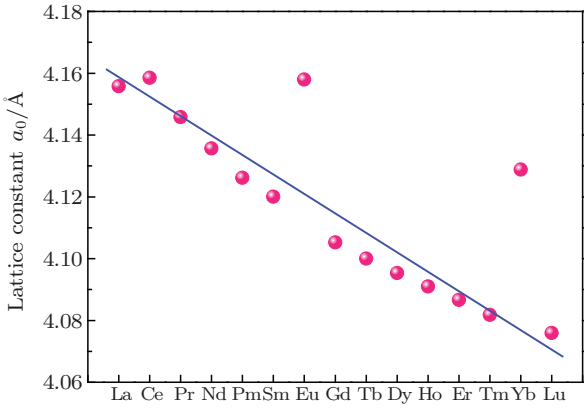


**Fig. 2.** (color online) The change of lattice parameter $a_0$ with the atomic number of *Ln* atoms in $Ln$B$_6$.

experimental values in Table 1, with a difference within 3%. This elucidates that the present calculations are reasonable and reliable. The $LnB_6$ compounds tend to decrease in size as going down the lanthanide series as shown in Fig. 2. We refer to this effect as the lanthanide contraction. While we note that Eu- and Yb-containing systems do not follow the trends of the rest of the lanthanides. There is not enough data to compare with our results of the positional parameters $x$ but the changes can be neglected, and they are all approximately equal to 0.2 Å. The positional parameters $x$ of $EuB_6$ and $YbB_6$ are larger than those of the others and closer to the "equal distance" of 0.2070 Å.[31] The abnormal behaviors of Eu and Yb are probably due to their special electronic configurations.

**Table 1.** Calculated lattice parameters $a_0$, positional parameter of boron atoms $x$, bulk modulus $B_0$, equilibrium volume $V$, pressure derivative $B_0'$, and independent elastic constants $C_{11}$, $C_{12}$, $C_{44}$ for $LnB_6$ accompanied with other calculated and experimental results.

| | $a$/Å | $x$/Å | $B_0$/GPa | $V$/Å$^3$ | $B_0'$ | $C_{11}$/GPa | $C_{12}$/GPa | $C_{44}$/GPa |
|---|---|---|---|---|---|---|---|---|
| $LaB_6$ | 4.1557 | 0.1998 | 173.6 | 71.77 | 3.72 | 473 | 24 | 92 |
| Exp. | 4.1568[a] | | 172.0[a] | | | 453[b] | 18[b] | 90[b] |
| Cal. | 4.1277[c] | 0.1997[c] | 180.0[c] | | 3.79[c] | 466[c] | 37[c] | 88[c] |
| $CeB_6$ | 4.1585 | 0.2001 | 173.5 | 71.91 | 3.73 | 460 | 31 | 82 |
| Exp. | 4.1360[d] | | 191.0[e] | | | 472[e] | 53[e] | 78[e] |
| Cal. | 4.1542[c] | 0.2002[c] | 173.0[c] | | 3.91[c] | 452[c] | 34[c] | 98[c] |
| $PrB_6$ | 4.1458 | 0.1998 | 173.8 | 71.26 | 3.72 | 463 | 30 | 75 |
| Exp. | 4.1260[d], 4.1300[f] | | | | | 474[e] | 44[e] | 45[e] |
| $NdB_6$ | 4.1357 | 0.1996 | 174.0 | 70.73 | 3.70 | 464 | 30 | 69 |
| Exp. | 4.1190[d], 4.1280[g] | | | | | | | |
| $PmB_6$ | 4.1262 | 0.1994 | 174.0 | 70.25 | 3.69 | 465 | 29 | 62 |
| $SmB_6$ | 4.1200 | 0.1993 | 174.1 | 69.94 | 3.71 | 465 | 29 | 56 |
| Exp. | 4.1330[g] | | 166.0[h] | | | 417[h] | –67[h] | 48[h] |
| $EuB_6$ | 4.1580 | 0.2020 | 152.4 | 71.89 | 3.59 | 434 | 11 | 69 |
| Cal. | 4.1485[i] | 0.2030[j] | 159.0[i] | | | | | |
| Exp. | 4.1780[g] | | | | | 415[k] | 42[k] | 60[k] |
| $GdB_6$ | 4.1053 | 0.1990 | 174.2 | 69.19 | 3.66 | 465 | 29 | 48 |
| Exp. | 4.1066[l], 4.1120[g] | | | | | 467[e] | 27[e] | 43[e] |
| Cal. | | | 175.0[i] | | | | | |
| $TbB_6$ | 4.1000 | 0.1989 | 174.1 | 68.92 | 3.65 | 465 | 29.3 | 43 |
| Exp. | 4.1050[m] | | | | | | | 37[e] |
| $DyB_6$ | 4.0953 | 0.1987 | 174.1 | 68.68 | 3.64 | 463 | 30 | 38 |
| Exp. | 4.0970[m] | | | | | | | |
| $HoB_6$ | 4.0910 | 0.1987 | 174.0 | 68.47 | 3.63 | 462 | 30 | 34 |
| Exp. | 4.0950[m] | | | | | 480[e] | 40[e] | 28[e] |
| $ErB_6$ | 4.0866 | 0.1986 | 174.0 | 68.25 | 3.64 | 460 | 31 | 29 |
| $TmB_6$ | 4.0818 | 0.1984 | 174.0 | 68.01 | 3.63 | 458 | 33 | 24 |
| $YbB_6$ | 4.1289 | 0.2014 | 152.6 | 70.39 | 3.54 | 447 | 6 | 44 |
| Cal. | 4.0790[i] | | | | | | | |
| Exp. | 4.1480[l] | | 153.0[h] | | | 335[h] | 81[h] | 40[h] |
| $LuB_6$ | 4.0760 | 0.1983 | 173.5 | 67.71 | 3.61 | 450 | 35 | 15 |

[a] Ref. [30], [b] Ref. [29], [c] Ref. [13], [d] Ref. [25], [e] Ref. [12], [f] Ref. [24], [g] Ref. [23], [h] Ref. [11], [i] Ref. [10], [j] Ref. [31], [k] Ref. [28], [l] Ref. [27], [m] Ref. [26].

### 3.2. Elastic properties

The most common assessment of mechanical properties can be made by the determination of the elastic constants. The elastic properties present valuable information about the mechanical and dynamical properties of crystals, the forces operating in solids, and they also provide important data for developing the interatomic potentials.[32,33] The elastic constants are identified as proportional to the second order coefficient in a polynomial and they can be derived from the energy variation by applying small strains to the equilibrium lattice configuration.[34] For the cubic structure, the independent elastic constants are $C_{11}$, $C_{12}$, and $C_{44}$,[31] which can be calculated through the following sets of strains: (i) $\varepsilon_{11} = \varepsilon_{12} = \delta$; (ii) $\varepsilon_{11} = \varepsilon_{22} = \varepsilon_{33} = \delta$; and, (iii) $\varepsilon_{12} = \varepsilon_{21} = \varepsilon_{13} = \varepsilon_{31} = \varepsilon_{23} = \varepsilon_{32} = \delta/2$. In the present work, we have calculated 15 sets of $\Delta E/V \sim \delta$ by varying $\delta$ from $-0.014$ to 0.014 in steps of 0.002. The results are listed in Table 1. As a comparison, the previous theoretical result and the available experimental data are also presented in Table 1. The published data on the elastic properties of hexaborides are scarce for most compounds, while there are ample experimental and theoretical results for $LaB_6$ and $CeB_6$. For $C_{11}$ and $C_{44}$, our results are in excellent agreement with others, while for $C_{12}$ the experimental and theoretical results given in the table demonstrate a large discrepancy among themselves. The origin of the large errors for $C_{12}$ can be understood because $C_{11}$ and $C_{12}$ are determined using

associated methods for both theoretical calculations and experiments. As $C_{11}$ is considerably larger than $C_{12}$, the large numerical error is consequently hard to avoid in the determination of $C_{12}$.[34] Obviously, the agreement between experiments and our calculations affirms the feasibility of our calculation scheme. The mechanical stability criterion[35] of the cubic lattice for elastic is $(C_{11}-C_{12})>0$, $C_{11}>0$, $C_{44}>0$, and $(C_{11}+2C_{12})>0$. As illustrated in Table 1, the elastic constants meet the criterion mentioned above, which indicates that all of the $Ln$B$_6$ are mechanically stable under zero pressure.

Since the elastic constants actually refer to a single crystal at microscopic scale and are normally not representative of the mechanical properties at larger length scales in actual applications, we turn to estimate the macroscopic parameters such as the shear modulus $G$ and the bulk modulus $B$.[36] The Voigt–Reuss–Hill (VRH)[37–39] approximation is an average of the two bounds, namely, the lower bound of Voigt and the upper bound of Reuss, which provides the best estimation for the mechanical properties of polycrystalline materials from the elastic constants. In the Voigt average,[38] the shear modulus and the bulk modulus of a cubic lattice are provided by

$$G_{\rm v}=[(C_{11}-C_{12})+3C_{44}]/5, \quad (1)$$

$$B_{\rm v}=(C_{11}+2C_{12})/3; \quad (2)$$

while in the Reuss average,[39] they are given by

$$5/G_{\rm R}=4\,(C_{11}-C_{12})^{-1}+3C_{44}^{-1}, \quad (3)$$

$$B_{\rm R}=(C_{11}+2C_{12})/3=B_{\rm v}. \quad (4)$$

Therefore, by Hill's empirical average,[37] the shear modulus and the bulk modulus of the polycrystalline material can be expressed as

$$G=(G_{\rm v}+G_{\rm R})/2, \quad (5)$$

$$B=(B_{\rm v}+B_{\rm R})/2. \quad (6)$$

We also obtain the static results for the bulk modulus $B_0$ and the pressure derivative of the bulk modulus $B_0'$ by fitting the static total energy versus lattice constant with the Birch–Murnaghan 3rd-order equation of states (EOS), which are listed in Table 1. The derived bulk modulus by fitting EOS turns out to be exactly the same as that from the above VRH approximation, as shown in Fig. 3, which again indicates that our calculations are consistent and reliable. In this work, the calculated bulk modulus is 173.6 GPa for LaB$_6$, which agrees well with the result of recent x-ray diffraction studies in Ref. [40], 173±7 GPa. For CeB$_6$, the present calculated value is 173.5 GPa, which is considerably close to the previous theoretical result 173 GPa.[13] For the sake of brevity, we do not enumerate the values one by one for other $Ln$B$_6$. As show in Fig. 3, only small differences appear between each other for the bulk modulus of a range of $Ln$B$_6$, which is due to lower $C_{12}$ compared with $C_{11}$. EuB$_6$ and YbB$_6$ are also outliers. In addition, according to Pugh's criterion,[41] the strength fracture is proportional to $B_0\times a_0$, where $B_0$ is the bulk modulus and $a_0$ is the lattice constant. Our calculated $B_0\times a_0$ is shown in Fig. 4. It can be seen that $B_0\times a_0$ is decreasing for the lanthanide hexaborides, indicating that the strength gets smaller and smaller.

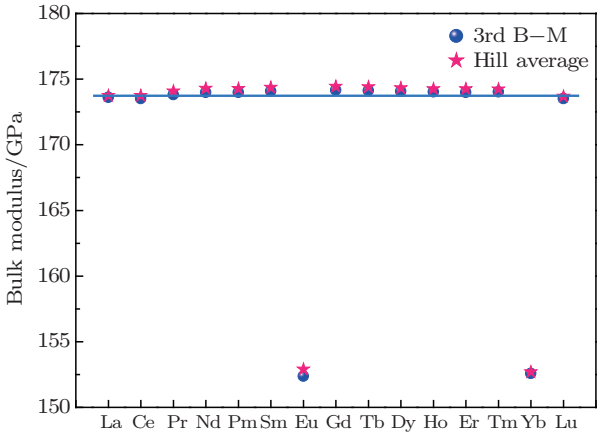


**Fig. 3.** (color online) The change of bulk modulus $B_0$ with the atomic number of $Ln$ atoms in $Ln$B$_6$. The pink points are derived according to Hill's empirical average theory and the blue points are obtained by fitting the Birch–Murnaghan 3rd-order equation of states.

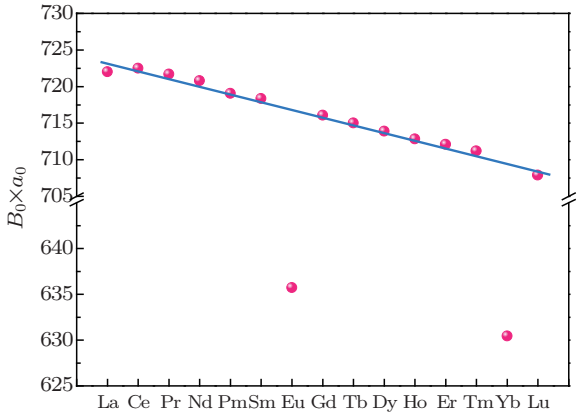


**Fig. 4.** (color online) Variation of $B_0\times a_0$ for $Ln$B$_6$ with the atomic number of $Ln$ atoms.

The single crystal shear moduli for the $\{100\}$ plane along the [010] direction and for the $\{110\}$ plane along the $[1\bar{1}0]$ direction are given by $G_{\{100\}}=C_{44}$ and $G_{\{110\}}=(C_{11}-C_{12})/2$,[42] respectively. These deformations correspond to a shear and reflect the degree of stability of the crystal with respect to a tetragonal shear. For all compounds, $G_{\{110\}}$ is found larger than $G_{\{100\}}$, indicating that it is easier to shear on the $\{100\}$ plane along the [010] direction than on the $\{110\}$ plane along the $[1\bar{1}0]$ direction. Figures 5 and 6 show that the Voigt's, Reuss's, and Hill's shear moduli decrease linearly with increasing atomic number of $Ln$ atoms except for EuB$_6$ and YbB$_6$. This tendency is similar to $C_{44}$ and is in accordance with the conclusion acquired in Ref. [12].

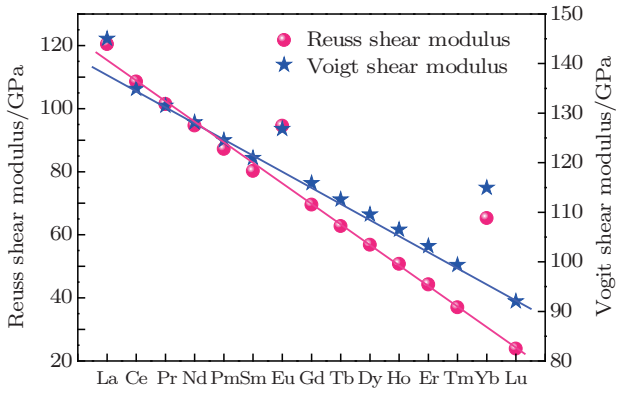


**Fig. 5.** (color online) The shear modulus $G$ for polycrystalline obtained according to Reuss and Voigt approximations, respectively.

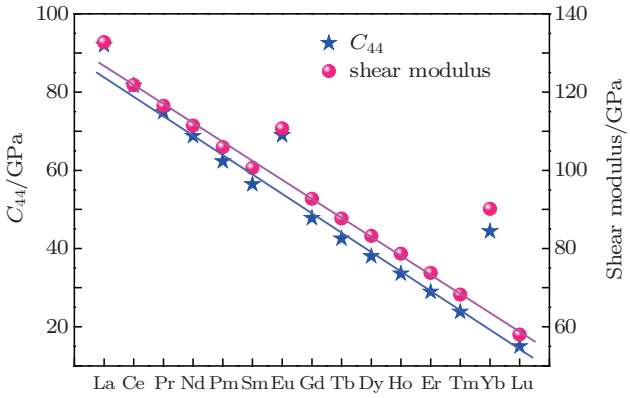


**Fig. 6.** (color online) The elastic constant $C_{44}$ for single crystal and the shear modulus $G$ for polycrystalline obtained based on Hill's approximations.

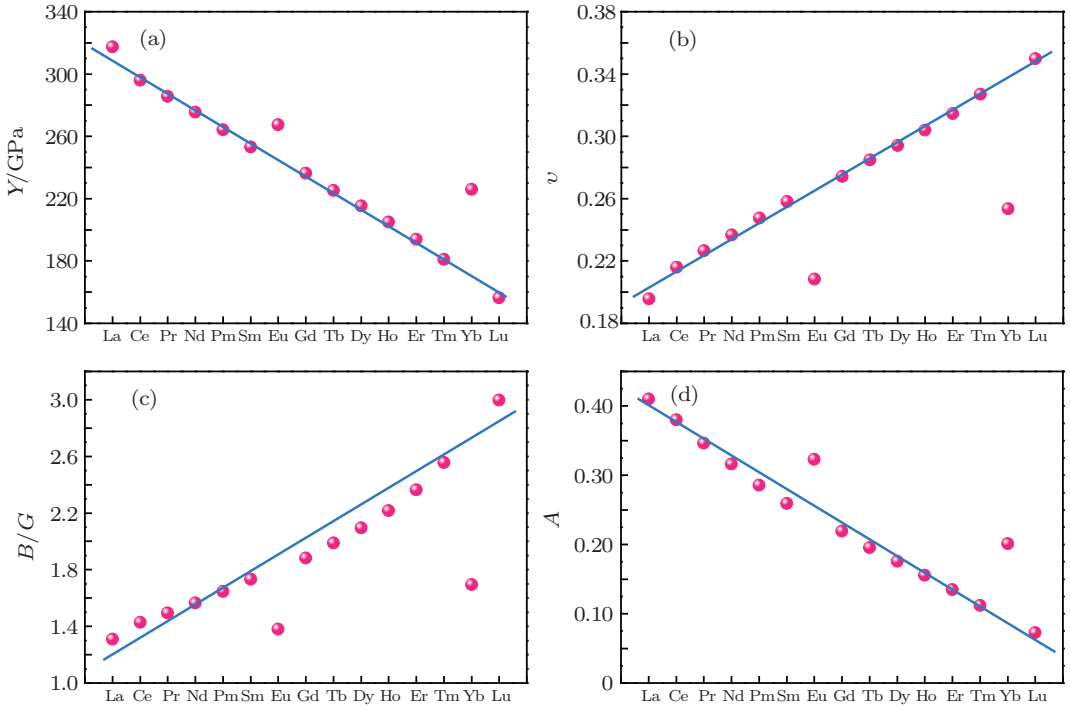


**Fig. 7.** (color online) (a) The Young's modulus $Y$, (b) the Poisson's ratio $\upsilon$, (c) $B/G$, and (d) Zener anisotropy factor $A$ estimated with Hill's approximation.

It is known that the Young's modulus, the Poisson's ratio, Zener anisotropy factor $A$, and the ratio of $B/G$ are the noteworthy parameters for materials in technology and engineering applications.[43] The results are plotted in Fig. 7. These parameters are calculated in terms of the elastic constants $C_{ij}$ via the following relations:

$$E = \frac{9BG}{3B+G}, \tag{7}$$

$$v = \frac{3B-2G}{2(3B+G)}, \tag{8}$$

$$A = \frac{2C_{44}}{C_{11}+C_{12}}. \tag{9}$$

The Young's modulus serves as a measurement of the stiffness of a solid and the Poisson's ratio evaluates the stability of a crystal against shear.[42] The relationship between the hardness and the Young's modulus is not identical for different materials: the general tendency is that the larger the modulus, the harder the material. The Young's modulus decreases with increasing atomic number, which demonstrates that the hardness is reduced gradually for the $Ln$B$_6$ compounds except for EuB$_6$ and YbB$_6$. The smaller Poisson's ratio indicates that $Ln$B$_6$ is relatively stable against shear.[36] Pugh[41] introduced the quotient of bulk to shear modulus of polycrystalline phases, where the shear modulus $G$ represents the resistance to plastic deformation while the bulk modulus $B$ represents the resistance to fracture. A high (low) $B/G$ corresponds to ductility (brittleness). The critical value which distinguishes ductile and brittle materials is about 1.75. Our calculated results are displayed in Fig. 7. The $B/G$ of $Ln$B$_6$ tends to increase with increasing atomic number except for EuB$_6$ and

$YbB_6$. The compounds lighter than $SmB_6$ present a brittle behavior, while the rest are ductile materials. $EuB_6$ and $YbB_6$ are still out of the tendency and they are brittle compounds. The Zener anisotropy factor $A$ is a measure of the degree of elastic anisotropy in a solid. The Zener anisotropy factor takes the value of 1 for a completely isotropic material. The calculated Zener anisotropy factor for $LnB_6$ is smaller than 1, which indicates that the compounds are entirely anisotropic.[42]

### 3.3. Debye temperature

The thermodynamic parameters such as the Debye temperature and the sound velocity are also essential physical parameters. In the present case, the Debye temperature $\theta_D$[44] is obtained with the calculated elastic constants according to the following relation:

$$\theta_D = \frac{h}{k}\left[\frac{3n}{4\pi}\left(\frac{N_A\rho}{M}\right)\right]^{1/3} v_m, \tag{10}$$

where $h$ is the Planck constant, $k$ is the Boltzmann constant, $N_A$ is the Avogadro number, $n$ is the number of atoms per formula unit, $M$ is the molecular mass per formula unit, and $\rho$ is the density.

**Table 2.** The calculated density ($\rho$), the longitudinal, transverse, mean elastic wave velocities ($v_l$, $v_t$, and $v_m$), and the Debye temperature ($\theta_D$) for $LnB_6$.

| | $\rho$/g·cm$^{-1}$ | $v_l$/m·s$^{-1}$ | $v_t$/m·s$^{-1}$ | $v_m$/m·s$^{-1}$ | $\theta_D$/K |
|---|---|---|---|---|---|
| $LaB_6$ | 4.714 | 8625 | 5306 | 5855 | 1110 |
| Cal. | | | | | 1165[a] |
| Exp. | 4.71[b] | | | | |
| $CeB_6$ | 4.733 | 8427 | 5072 | 5609 | 1062 |
| Exp. | 4.797[c] | | | | 751[d] |
| $PrB_6$ | 4.795 | 8288 | 4928 | 5457 | 1036 |
| $NdB_6$ | 4.908 | 8110 | 4764 | 5281 | 1005 |
| $PmB_6$ | 4.961 | 7974 | 4620 | 5127 | 979 |
| $SmB_6$ | 5.111 | 7768 | 4436 | 4929 | 942 |
| Exp. | 5.06[c] | | | | |
| $EuB_6$ | 5.009 | 7745 | 4701 | 5194 | 984 |
| Exp. | 4.895[c] | | | | |
| $GdB_6$ | 5.332 | 7476 | 4170 | 4642 | 891 |
| $TbB_6$ | 5.391 | 7350 | 4032 | 4495 | 864 |
| $DyB_6$ | 5.497 | 7203 | 3890 | 4342 | 835 |
| $HoB_6$ | 5.572 | 7077 | 3756 | 4198 | 808 |
| $ErB_6$ | 5.649 | 6946 | 3613 | 4043 | 779 |
| $TmB_6$ | 5.708 | 6816 | 3457 | 3874 | 748 |
| $YbB_6$ | 5.612 | 6973 | 4007 | 4451 | 849 |
| Exp. | 5.53[c] | | | | |
| $LuB_6$ | 5.882 | 6532 | 3139 | 3529 | 682 |

[a] Ref. [46], [b] Ref. [29], [c] Ref. [28], [d] Ref. [3].

The average sound velocity $v_m$ of materials can be obtained according to the following formula:

$$v_m = \left[\frac{1}{3}\left(\frac{2}{v_t^3} + \frac{1}{v_l^3}\right)\right]^{-1/3}. \tag{11}$$

For the cubic crystal, $v_l$ and $v_t$ are the longitudinal and the transverse elastic wave velocities, which can be obtained from the elastic modulus by the famous Navier's equations[45]

$$v_l = \left(\frac{B + 4G/3}{\rho}\right)^{1/2}, \tag{12}$$

$$v_t = \left(\frac{G}{\rho}\right)^{1/2}. \tag{13}$$

Based on these equations, we derive the corresponding values which are tabulated in Table 2. It can be seen that the sound velocity decreases from $LaB_6$ to $LuB_6$ except $EuB_6$ and $YbB_6$. As far as we know, there are no available experimental or theoretical values to compare with our results for these parameters. We believe that the Debye temperature we obtained for $LnB_6$ is reasonable in comparison with the theoretical Debye temperature for $LaB_6$ (1165 K)[46] at zero pressure.

### 3.4. Electronic structure

It is clear that the structural and elastic properties of the lanthanide series solid compounds change regularly, which is strongly related to the unique electron configuration of the lanthanide series atoms. From La to Lu, the valence electron

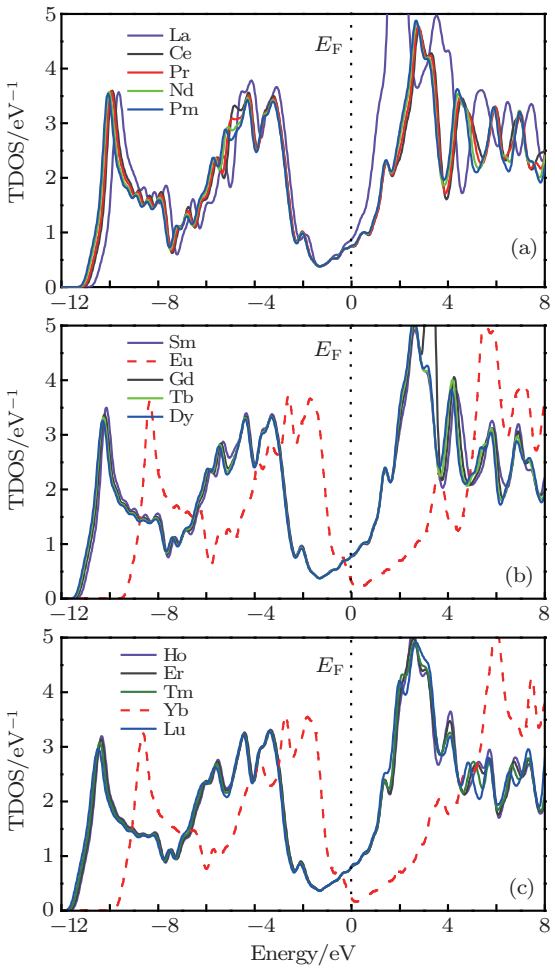


**Fig. 8.** (color online) Total electron density of states of $LnB_6$: (a) $Ln$ = La, Ce, Pr, Nd, Pm; (b) $Ln$ = Sm, Eu, Gd, Tb, Dy; (c) $Ln$ = Ho, Er, Tm, Yb, Lu.

configuration is $4f^{0-14}5d^{0-1}6s^2$ and electrons are added to the inner unfilled 4f shell continuously with the increasing atomic number, resulting in a continuous but minor change in the elemental properties. As can be seen from Fig. 8, the distribution of the total electronic density of states of $LnB_6$ is very similar. The total DOS demonstrates that there is a deep valley close to the Fermi level $E_F$ and this valley is referred to as a pseudogap. This pseudogap indicates the presence of a strong covalent bonding in the $B_6$ octahedron cage.[36] There is a relationship between the structural stability and the position of $E_F$ with respect to the pseudogap. From Fig. 8, we observe that the Fermi level falls below the pseudogap in $EuB_6$ and $YbB_6$ while is above the pseudogap in the other compounds. This indicates that not all of the bonding states are filled and some extra electrons are required to reach the maximum stability for $EuB_6$ and $YbB_6$. This phenomenon is consistent with the lower bulk moduli of $EuB_6$ and $YbB_6$.

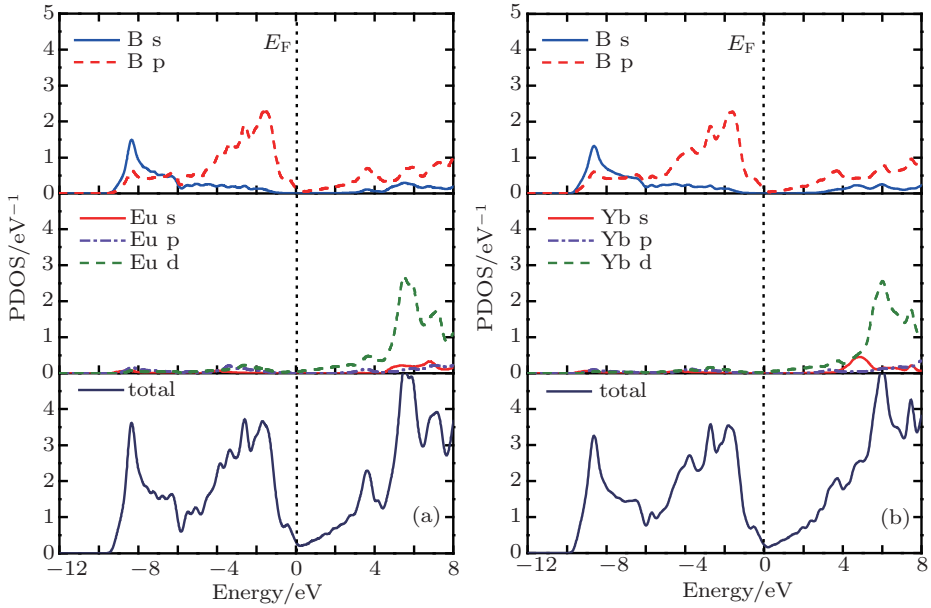


**Fig. 9.** (color online) Total and angular-momentum-projected densities of states of (a) $EuB_6$ and (b)$YbB_6$.

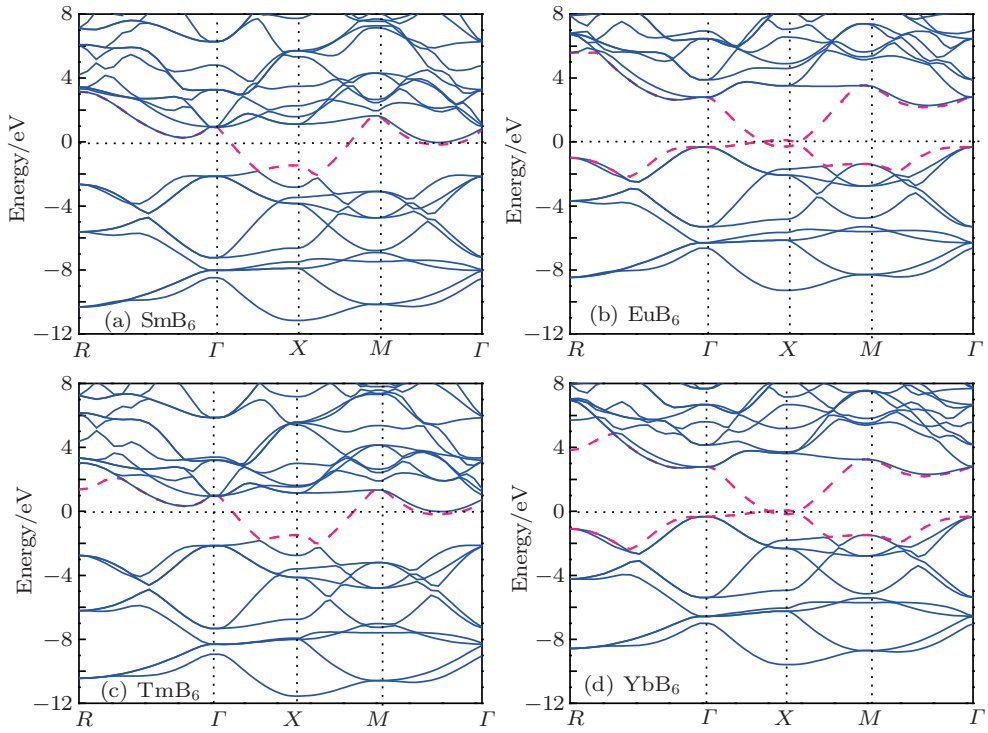


**Fig. 10.** (color online) Energy band structure along the principal high-symmetry directions in the Birllouin zone for (a) $SmB_6$, (b) $EuB_6$, (c) $TmB_6$, and (d) $YbB_6$ in the stable structure.

In Fig. 9, the total and the partial densities of states (PDOS) are presented for $EuB_6$ and $YbB_6$. The B 2s and 2p hybridization controls the lower bonding peak located at the energy of approximately −14 eV below the Fermi level.[47] Such states are typical for all $CaB_6$ like hexaborides. The B 2s and 2p interactions from intraoctahedron contribute mainly to the upper bonding peaks in the energy range from −10 eV to −6 eV. The upper subgroup, which ranges from −6 eV to the Fermi level, is composed of B 2p orbitals. The contributions are primarily from the interoctahedral bonds except for the range very close to the Fermi level where the intraoctahedral B–B bonds again become important. However, both the B-p and *Ln*-d states are spread out on both sides of the Fermi level. For the sake of simplicity, we only display the calculated band structures of $SmB_6$, $EuB_6$, $TmB_6$, and $YbB_6$ along the high symmetry directions in the Brillouin zone in Fig. 10. As we can see, there are dramatic differences between $SmB_6$ and $EuB_6$, and the same as to $TmB_6$ and $YbB_6$. It is amazing to find that small gaps may exist in $EuB_6$ and $YbB_6$, and both of them possess higher internal parameters $x$ (see Table 1). As illustrated in Fig. 9, the band overlap in the Fermi level happens between the B-s and *Ln*-d states; and as $x$ increases, the *Ln* atoms are further apart from the B cages, which leads to the raise of the dispersed conduction band. The intra-cage bonding states go down in energy, resulting in the opening of a small gap.

## 4. Conclusion

The lattice constants, elastic properties, and electronic structures of $LnB_6$ ($Ln$ = La, Ce, ..., Yb, Lu) have been studied comprehensively by the PAW method within the GGA. The *ab initio* calculated lattice constants and the elastic properties are in good agreement with the experimental data and other theoretical results available.

The lattice constants are compressed from $LaB_6$ to $LuB_6$ due to the famous lanthanide contraction effect. The independent elastic constants are investigated and the bulk moduli, shear moduli, Young's moduli, Poisson's ratios, and Zener anisotropy factors are also estimated for the $LnB_6$ polycrystals. Our results show that the change of the shear modulus is similar to that of $C_{44}$ and the hardness reduces gradually from $LaB_6$ to $LuB_6$. The analysis of the electronic density of states indicates the presence of a pseudogap. The total densities of states of $EuB_6$ and $YbB_6$ shift towards higher energy, which is inconsistent with their lower bulk moduli. We predict the Debye temperatures for $LnB_6$ and they gradually decrease except for $EuB_6$ and $YbB_6$. The compounds of the divalent *Ln* elements Eu and Yb are usually exceptions to the trends, which holds mainly for the adoption of their divalent configurations due to their special electron configurations. Since there are no experimental data available for some of these parameters, we believe that our calculated results also provide a reference for future experimental work.

## References


[1] Kauer E 1963 *Phys. Lett.* **7** 171
[2] Vandenberg J M, Matthias B T, Corenzwit E and Barz H 1975 *Mater. Res. Bull.* **10** 889
[3] Lüthi B, Blumenröder S, Hillebrands B, Zirngiebl E, Güntherodt E and Winzer K 1984 *Z. Phys. B Condens. Matter* **58** 31
[4] Xu N, Shi X, Biswas P K, Matt C E, Dhaka R S, Huang Y, Plumb N C, Radovi M, Dil J H, Pomjakushina E, Conder K, Amato A, Salman Z, Paul D M, Mesot J, Ding H and Shi M 2013 *Phys. Rev. B* **88** 121102
[5] Wolgast S, Kurdak Ç, Sun K, Allen J W, Kim D J and Fisk Z 2013 *Phys. Rev. B* **88** 180405(R)
[6] Weng H M, Zhao J Z, Wang Z J, Fang Z and Dai X 2014 *Phys. Rev. Lett.* **112** 016403
[7] Baranovskiy A E, Grechnev G E, Fil V D, Ignatova T V, Logosha A V, Panfilov A S, Svechkarev I V, Shitsevalova N Y, Filippov V B and Eriksson O 2007 *J. Alloys Compd.* **442** 228
[8] Wang L, Luo G F, Valencia D, Sierra Llavina C H, Sabirianov R F, Lu J, Lu J Q, Mei W N and Cheung C L 2013 *J. Appl. Phys.* **114** 143709
[9] Yu Y, Chen C L, Zhao G D, Zheng X L and Zhu X H 2014 *Chin. Phys. Lett.* **31** 106301
[10] Grechnev G E, Baranovskiy A E, Fil V D, Ignatova T V, Kolobov I G, Logosha A V, Shitsevalova N Y, Filippov V B and Eriksson O 2008 *Low Temp. Phys.* **34** 921
[11] Takegahara K, Kasaya M, Goto T and Kasuya T 1985 *Phys. B+C* **130** 49
[12] Nakamura S, Goto T, Kunii S, Iwashita K and Tamaki A 1994 *J. Phys. Soc. Jpn.* **63** 623
[13] Gürel T and Eryiğit R 2010 *Phys. Rev. B* **82** 104302
[14] Gao M C, Rollett A D and Widom M 2007 *Phys. Rev. B* **75** 174120
[15] Kresse G and Joubert D 1999 *Phys. Rev. B* **59** 1758
[16] Blöchl P E 1994 *Phys. Rev. B* **50** 17953
[17] Kresse G and Hafner J 1993 *Phys. Rev. B* **47** 558(R)
[18] Kresse G and Furthmüller J 1996 *Comput. Mater. Sci.* **6** 15
[19] Kresse G and Furthmüller J 1996 *Phys. Rev. B* **54** 11169
[20] Monkhorst H J and Pack J D 1976 *Phys. Rev. B* **13** 5390
[21] Issa A, Saal J E and Wolverton C 2014 *Acta Mater.* **65** 240
[22] Birch F 1947 *Phys. Rev.* **71** 809
[23] Singh N, Saini S M, Nautiyal T and Auluck S 2007 *J. Phys.: Condens. Matter* **19** 346226
[24] Walker H C, McEwen K A and McMorrow D F 2009 *Phys. Rev. B* **79** 054402
[25] Zhang M F, Wang X Q, Zhang X W, Wang P F, Xiong S L, Shi L and Qian Y T 2009 *J. Solid State Chem.* **182** 3098
[26] Takahashi K and Kunii S 1997 *J. Solid State Chem.* **133** 198
[27] Blomberg M K, Merisalo M J, Korsukova M M and Gurin V N 1995 *J. Alloys Compd.* **217** 123
[28] Zherlitsyn S, Wolf B, Lüthi B, Lang M, Hinze P, Uhrig E, Assmus W, Ott H R, Young D P and Fisk Z 2001 *Eur. Phys. J. B* **22** 327
[29] Tanaka T, Yoshimoto J, Ishii M, Bannai E and Kawai S 1977 *Solid State Commun.* **22** 203
[30] Lundström T, Lönnberg B, Törmä B, Etourneau J and Tarascon J M 1982 *Phys. Scr.* **26** 414
[31] Massidda S, Continenza A, Pascale T M de and Monnier R 1997 *Z. Phys. B* **102** 83
[32] Yan X Z, Kuang X Y, Mao A J, Kuang F G, Wang Z H and Sheng X W 2013 *Acta Phys. Sin.* **62** 107402 (in Chinese)
[33] Qi C J, Feng J, Zhou R F, Jiang Y H and Zhou R 2013 *Chin. Phys. Lett.* **30** 117101
[34] Wang S Q and Ye H Q 2003 *J. Phys.: Condens. Matter* **15** 5307
[35] Sin'ko G V and Smirnow N A 2002 *J. Phys.: Condens. Matter* **14** 6989

[36] Ravindran P, Fast L, Korzhavyi P A, Johansson B, Wills J and Eriksson O 1998 *J. Appl. Phys.* **84** 4891

[37] Hill R 1952 *Proc. Phys. Soc. A* **65** 349

[38] Voigt W 1928 *Lehrbuch der Kristallphysik* (B. G. Teubner: Leipzig)

[39] Reuss A and Angew Z 1929 *Math. Mech.* **9** 55

[40] Godwal B K, Petruska E A, Speziale S, Yan J, Clark S M, Kruger M B and Jeanloz R 2009 *Phys. Rev. B* **80** 172104

[41] Pugh S F 1954 *Philos. Mag.* **45** 823

[42] Yang J W, Gao T and Gong Y R 2014 *Solid State Sci.* **32** 76

[43] Cai T, Zhang Z J, Zhang P, Yang J B and Zhang Z F 2014 *J. Appl. Phys.* **116** 163512

[44] Anderson O L 1963 *J. Phys. Chem. Solids* **24** 909

[45] Sa B S, Zhou J and Sun Z M 2012 *Intermetallics* **22** 92

[46] Xu G L, Chen J D, Xia Y Z, Liu X F, Liu Y F and Zhang X Z 2009 *Chin. Phys. Lett.* **26** 056201

[47] Mogulkoc Y, Ciftci Y O, Kabak M and Colakoglu K 2014 *Superlattices Microstruct.* **71** 46